Constellation designs for improved error correction in 5G MIMO systems under correlated Nakagami-m fading

A Graduate Project Report submitted to Manipal Academy of Higher Education in partial fulfilment of the requirement for the award of the degree of

BACHELOR OF TECHNOLOGY

In

Electronics and Communication Engineering

Submitted by

Vibhuti Ravi

Reg. No.: 170907092

Under the guidance of

Dr. Goutham Simha G D

Manipal Institute of Technology

DEPARTMENT OF ELECTRONICS AND COMMUNICATION ENGINEERING

MANIPAL INSTITUTE OF TECHNOLOGY

MANIPAL

(A constituent unit of MAHE, Manipal)

MANIPAL-56104, KARNATAKA, INDIA

JUNE 2021

DEPARTMENT OF ELECTRONICS AND COMMUNICATION ENGINEERING

MANIPAL INSTITUTE OF TECHNOLOGY

(A Constituent College of MAHE)

MANIPAL – 576104, KARNATAKA, INDIA

Manipal
2nd June, 2021

CERTIFICATE

This is to certify that the project titled **"Constellation Designs for improved error correction in 5G MIMO systems under correlated Nakagami-m fading"** is a record of the bonafide work done by **Vibhuti Ravi** (Reg. No. **170907092**) submitted in partial fulfilment of the requirements for the award of the Degree of Bachelor of Technology (B.Tech) in **Electronics and Communication Engineering** of Manipal Institute of Technology, Manipal, Karnataka (A Constituent unit of Manipal Academy of Higher Education), during the academic year 2020 – 2021.

INTERNAL GUIDE

Dr. Goutham Simha G D
Assistant Professor, ECE
M.I.T Manipal

Prof. Dr. G. Subramanya Nayak

HOD, ECE
M.I.T Manipal

ACKNOWLEDGEMENTS

The satisfaction that accompanies the successful completion of any task would be incomplete without mention of the people who had been of great help to me in making this possible.

I would like to express my sincere gratitude to Dr. Goutham Simha G D, my guide, for his continued support, guidance and motivation at every phase of this project. He always took time to give me valuable suggestions and feedback throughout this project. I am very fortunate to have him as my guide and I sincerely thank him for the same.

I would like to thank Dr. D Srikanth Rao, Director of MIT, Manipal for giving us such a good opportunity to have practical exposure. I am grateful to Dr. G. Subramanya Nayak and Dr. Bore Gowda without whose help this project would not have been possible.

I wish to thank the project review committee members, Dr. Anu Shaju Areeckal, Dr. Datta Guru V. Kamath, Dr. Aparna U. and Ms. Aparna V who, amidst their busy schedule, were able to give me valuable feedback and suggestions in improving the presentation of this project.

I also wish to express a deep sense of gratitude to my beloved parents and friends for their support, strength and help.

ABSTRACT

In today's world where two-thirds of all IP traffic comes from wireless and mobile devices and with around 20.4 billion Internet of Things devices connected around the world, there has been a huge focus on innovation in the wireless industry with no signs of slowing down. With the advent of 5G technology, several techniques are being investigated for deployment in fifth generation of mobile service applications. A big part of this is Spatial Modulation (SM) Multiple-input multiple-output (MIMO) which gives a high spectral efficiency. In order to achieve a better performance and overcome the inherent throughput loss of conventional SM, a new SM scheme, referred to as Enhanced SM (ESM) has been introduced. The objective of the project is to study the performance of ESM systems under correlated Nakagami fading channels.

The main objective is to evaluate the Symbol Error Rate (SER) vs E_b/N_o performances of ESM systems of different configurations with varying spectral efficiencies under correlated Nakagami-m fading. In order to build the ESM system, ESM constellation designs using geometric interpolation are implemented. The incoming bits are then mapped to a constellation/ antenna index according to ESM mapping. The transmitted symbols are sent over a correlated Nakagami-m fading channel using the Kronecher correlation model for spatially correlated MIMO systems. SER vs E_b/N_o of this system is plotted and analysed for different m values. Further, grouping techniques have been used to improve the system performance and overcome high channel correlation in MIMO systems. Various SM schemes have been looked at to study their performance compared to ESM under the same fading channels.

The results for the ESM system under correlated Nakagami-m fading channel indicated that an increase in the shape factor m resulted in lower signal correlation gives lesser symbol error rate. On studying how significantly the channel phase distribution affects the performance of ESM MIMO systems, it was seen that the assumption of the channel phase distribution has a major impact on the performance and that it is shown that uniform assumption of channel phase distribution is incorrect and leads to erroneous conclusions. The results for comparison of various SM schemes indicated that the same spectral efficiency and transmit power, ESM performs better than GSM (General Spatial Modulation) and SM schemes.

In conclusion, the work is a comprehensive study on ESM MIMO systems and will help highlight the advantages of ESM techniques under a generalized fading channel i.e. the Nakagami-m fading channel. Matlab 2019 is used to carry out the simulations and evaluate the performances.

LIST OF TABLES

LIST OF FIGURES

Contents

CHAPTER 1
INTRODUCTION

1.1. Introduction

This chapter shall introduce the current scenario in the space of MIMO communications and highlight the significance of Spatial Modulation techniques. The motivation of introducing Enhanced Spatial Modulation (ESM) is then brought in followed by the key objectives and target specifications of this project.

It comes as no surprise that there has been an explosive increase in the number of wireless client devices. There has been a plethora of technological advancements made to accommodate these requirements by providing high throughput. This led to a surge of research activities in the field of Multiple-input multiple-output (MIMO) and is presently one of the most dynamic areas of research. Also, the significant progress in very-large-scale integration (VLSI) technology enabled complex signal processing algorithms with small area devices and low power consumption. This led to the development of various communications techniques in the past decade.

1.2. Present day scenario

Due to the skyrocketing demand for higher data rates, energy and spectral efficiency, there is an immense need of new spectrum and energy efficient physical layer technologies. Among the set of existing technologies, MIMO systems promise a boost in the spectral efficiency by simultaneously transmitting data from multiple transmit antennas to the receiver. MIMO, however is not highly energy efficient due to large power consumption by active antennas. In order to achieve the spectral and energy efficiency of next generation wireless communications, a group of MIMO techniques, called space modulation techniques (SMTs) has emerged.

In SMTs, a new spatial constellation diagram is included to increase the spectral efficiency but also saving energy resources and reducing receiver computational complexity. [1] Here, the inherent antenna redundancy is exploited using a concept called spatial modulation (SM). Unlike the traditional modulation schemes, SM conveys information by making use of the multipath nature of the MIMO fading channel as an extra constellation diagram referred to as spatial constellation. Therefore, here the active antenna indices are also used to transmit information.

1.3. Motivation

There are several limitations to MIMO systems, however, with regards to the decoding complexity, which increases with the number of antennas. A lesser number of radio-frequency (RF) chains in the transmitter than the number of antennas is used to minimize the cost and energy consumption. [1] In order to overcome these limitations, we use space modulation techniques (SMTs) where we increase the spatial efficiency and reduce the complexity and energy used. This is done by adding a new spatial constellation diagram and exploiting the inherent antenna redundancy. By using the multipath nature of the MIMO systems, SM uses an extra constellation diagram referred to as spatial constellation in addition to using the indices of active antennas to convey information.

In today's applications, we require schemes that achieve high throughput and performance. This requirement and the inherent throughput loss of conventional SM are the main motivations to introduce a new SM scheme, referred to as Enhanced SM (ESM). ESM is a novel Spatial Modulation technique that uses combinations of antenna indexes and constellation types to increase the throughput compared to standard Spatial Modulation. In the designs used in this project, secondary signal constellations obtained by one geometric interpolation from the primary signal constellation plane is used. [2]

The main feature of ESM is that a symbol from the primary constellation on one antenna and a symbol from the secondary constellation on the other is transmitted. The secondary signal constellations are derived from the primary constellation by means of geometric interpolation in the signal space, which leads to a significant increase of the number of active antenna and modulation combinations used. [2] The end result would show that good system performance can be achieved with the advanced MIMO technique and that ESM provides a significant performance gain with respect previous methods.

1.4. Objective

The main objective is to evaluate the Symbol Error Rate (SER) vs E_b/N_o performances of ESM systems of different configurations with varying spectral efficiencies under correlates Nakagami fading. Further, various SM schemes will be looked at to study their performance compared to ESM under the same fading channels.

The work will also include a study on how significantly the channel phase distribution affects the performance of ESM MIMO systems by carrying out simulations of the ESM system over uniform and non-uniform phase generalized fading models.

Further, the Enhanced Spatial Modulation schemes with transmit antenna grouping will be developed where the transmit antennas are divided into equal sized groups and one antenna from each group is used to carry out Enhanced Spatial Modulation. Two grouping techniques called block and interleaved grouping will be used to further improve the performance of this system over correlated channels.

In conclusion, the work will be a study on ESM MIMO systems and will help highlight the advantages of ESM techniques under a generalized fading channel i.e. the Nakagami-m fading channel.

1.5. Project work schedule

January 2021	• Generated ESM Constellation Diagram
February 2021	• Simulated performance of 4x4 ESM for correlated Nakagami-m channel
March 2021	• Conducted analysis for 4x4 ESM under Nakagami-m with exact phase, and with uniform phase distributions. • Generalized ESM and plotted performance of 8x4 ESM for correlated Nakagami-m channel with antenna grouping.
April 2021	• Compared performance of ESM with GSM and SM for 8x4 and 4x4 under Nakagami-m fading • Performance simulation of ESM MIMO system over correlated Nakagami-m for 16x4 system with antenna grouping.
May 2021	• Comparison with 16x4 SM, GSM for correlated and uncorrelated Nakagami-m fading. • Performance Analysis • Case study on High-altitude platform systems • Documentation

1.6. Organization of the project report

This report is organized into five chapters. Chapter 2 introduces the concepts of MIMO system model, Spatial Modulation, Nakagami fading channel, spatial correlation and antenna grouping. Chapter 3 gives the design procedure for ESM and the methodology followed. Chapter 4 discussed the results obtained from the simulations performed of the communication systems developed in Matlab. Chapter 5 provides a case study on High Altitude Platforms. Chapter 6 provides a summary of the work, the conclusions and suggestions for future studies.

CHAPTER 2
BACKGROUND THEORY

2.1. Introduction

This chapter shall introduce the MIMO system model. The concept of spatial modulation is thoroughly discussed in this chapter. The Nakagami-m channel model and its key equations has been discussed. Finally, the Kronecker correlation model is described as well as a brief overview of spatial correlation and antenna grouping.

2.2. MIMO System Model

Due to its performance enhancing capabilities, MIMO (Multiple-input Multiple-output) has gained a lot of popularity in recent times. Multipath fading which is due to the difference on the angles of arrival, time delays and differing frequencies acts as an impairment in wireless communication. Because of this, the received signal fluctuates in time or frequency or space. This is called fading and it severely affects the performance of a wireless communication system. MIMO is a technique which severely helps with these problems as well as resource constraints by exploiting the spatial dimension provided by the multiple transmit and receive antennas. The performance gain obtained by using MIMO is due to array gain, spatial diversity gain, spatial multiplexing gain and interference reduction.

In wireless communications, a transmitter communicates with a receiver through free-space medium. Depending on the number of antennas at both transmitter and receiver, several link configurations can be found. The simplest configuration is single-input single-output (SISO), where both transmitter and receiver each equipped with single antenna. [1] If both transmitter and receiver have multiple antennas, a multiple-input multiple-output (MIMO) configuration is established. In Figure 2.1 shows the basic building blocks of a MIMO system model with N_t transmit antennas and N_r receive antennas is depicted. The source bits have to be mapped to data symbols such as Quadrature Amplitude Modulation. This signal then has to pass through the encoder where Spatial Modulation, Quadrature Spatial Modulation etc. are applied. These signals propagate from the transmit antenna to receive antenna through the medium. The receiver then reverses the transmit operations to obtain the sink bits.

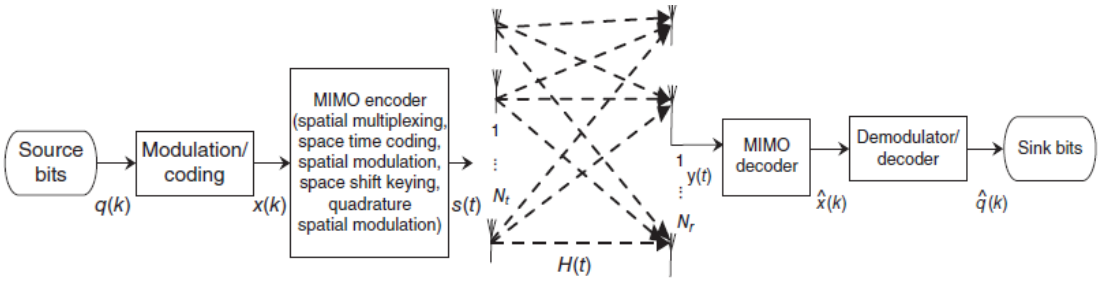

Fig 2.1. General MIMO system model

Source: [1] Space modulation techniques by Raed Mesleh, Abdelhamid Alhassi, 2018 JohnWiley & Sons, Inc

For a MIMO system with N_R number of receive antennas and N_T number of the transmit antennas, the MIMO system can be modelled as depicted in Eqn. 2.1 [1],

$$\begin{bmatrix} y_1 \\ y_2 \\ \vdots \\ y_{Nr} \end{bmatrix} = \begin{bmatrix} h_{11} & \cdots & h_{1Nt} \\ \vdots & \ddots & \vdots \\ h_{Nr1} & \cdots & h_{NrNt} \end{bmatrix} \begin{bmatrix} x_t^1 \\ x_t^2 \\ \vdots \\ x_t^{Nt} \end{bmatrix} + \begin{bmatrix} n_1 \\ n_2 \\ \vdots \\ n_{Nr} \end{bmatrix} \tag{2.1}$$

which can be expressed as,

$$\mathbf{y = Hs + n} \tag{2.2}$$

In (2.2), H is the $N_R \times N_T$ channel matrix where $h_{m,n}$, is the channel gain between the mth receive antenna and the nth transmit antenna. s is the $N_T \times 1$ transmitted signal vector with normalized power, i.e., $s = \sqrt{x} / Es$, and n is the additive white Gaussian noise (AWGN). The AWGN noise is a complex Gaussian noise that is temporally and spatially white with zero mean and a covariance matrix of $\sigma^2_n I_{Nr}$, where $\sigma^2_n = N_0 B$, with N_0 denoting the noise power spectral density and B is the channel bandwidth. [1]

At the receiver, the optimum maximum-likelihood (ML) detector can be used to decode the transmitted messages as given in Eqn. 2.3,

$$\hat{x} = \arg\min_{x_i \in X} \left\| y - \tilde{H} x_i \right\|^2_{\mathrm{F}} \tag{2.3}$$

Where $\hat{x}$ denotes the estimated transmitted symbol, $\widehat{H}$ is the estimated channel matrix at the receiver, $|| \cdot ||_F$ is the Frobenius norm, and x_i is a possible transmitted vector from a set containing all possible transmitted vectors combinations between transmit antennas and data symbols.

The ML decoder in (2.3) looks through all the transmitted vectors and picks the vector that is closest to the received signal vector y. That vector is chosen to be the most probable transmitted vector. The closer the two vectors from the set *X* to each other's, the higher the probability of error. Therefore, while designing the constellation diagram, it is better to place the vectors as far apart from each other as possible. This can be done also through proper design of the MIMO channel matrix H. Also, the computational complexity of encoding and decoding should be practical, systems with higher complexity tends to perform better.

Channel modelling is important in order to calculate the different performance metrics of the wireless channel and analyse if the performance fits the requirements. Since the received signal is assumed to be a sum of all the multipath components from different obstacles between transmitter and receiver. If the channel gains are modelled as Gaussian, the channel follows Rayleigh distribution. There are several generalised fading models as well. In particular, Nakagami-m which will be discussed further.

2.3. Spatial Modulation

In this sub section, the concept of Space Modulation Techniques is introduced using some examples. This is a unique MIMO transmission scheme that uses the different channel paths to convey additional information bits. One or more antennas are turned on for a specific interval of time while the others are turned off. The advantage of these systems is that we are able to design transmitters with a single RF chain resulting in cost reduction, low computational complexity and high-energy efficiency. [3] We make use of the Euclidian difference among the various channel vectors to transmit co-channel signals, thereby increasing the data rate.

The active transmit antenna changes every channel use depending on the incoming bits. The incoming bits are mapped to antenna indices using transmit antenna switching. Therefore, the information bits get mapped to a three- dimensional constellation diagram. In addition to the two-dimensional QAM constellation diagram, a third dimension is provided by the antenna-array where the incoming bits are mapped onto transmit antennas. In spatial modulation (SM), the additional bits are mapped onto a "SM constellation diagram", where each constellation element is constituted by either a single one or a subset of antenna-elements. In SM, a single RF chain is used since there is one active antenna in every time slot. Fig 2.2 shows an example of SM constellation diagram. Here, *Nt* i.e. transmit antennas and *Nr* i.e. receive antennas are both chosen to be 4. At the receiver, ML decoder is considered. If the block of bits to be encoded is "1100". The first log_2

(N_t)= 2 bits, "11," determine the single active transmit antennas (Transmit antenna 3), while the second $log_2 (M)$ = 2 bits, "00," determine the transmitted PSK/QAM symbol. [1]

Using this example, we assume that $q = [\,0\ 1\ 1\ 0\,]^T$ input bits are to be transmitted at a particular time instant using SM. The first group of data bits [0 1] determines the antenna index say, l=2. The second group of data bits [0 1] would determine the symbol say $S3$ = -1-j according to the QPSK constellation diagram selected. [1] The resultant symbol vector would now become $x_t^{RF}(t) = [0\ -cos(w_c t)\text{-}sin(w_c t)\ 0\ 0]^T$. The overall spectral efficiency is equal to $log_2 N_t + log_2 M$. We are thus able to increase the spectral efficiency and attain higher energy-efficiency.

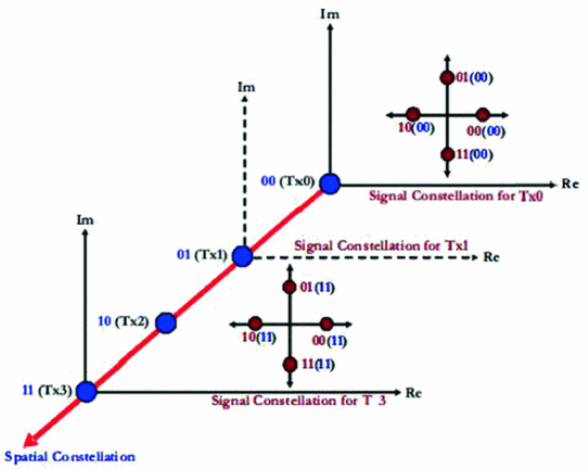

Fig. 2.2. An example of SM constellation diagram

Source: [1] Space modulation techniques by Raed Mesleh, Abdelhamid Alhassi, 2018 JohnWiley & Sons, Inc

One advantage of SM is that interchannel interference (ICI) can be totally avoided since only antenna is active at a time. Additionally, transmit antenna synchronization is not required and the ML receiver complexity is also much less that other MIMO techniques while improving the energy efficiency.

2.4. Nakagami-m channel model

As mentioned earlier, the signal though the communication medium always suffers from multipath effects and fading. The Rayleigh and Rician distributions are usually used to model channels over small geographical areas or short term fades. For wider areas, the log-normal distribution is employed. Rayleigh however falls short in describing long-distance fading effects with sufficient accuracy. This was observed by M. Nakagami who came up with a parametric gamma function to

fit the empirical values he obtained from his large-scale experiments on rapid fading in high frequency long-distance propagation. Although empirical, the formula is rather elegant. This can model a variety of fading environments including those modelled by the Rayleigh and one-sided Gaussian distributions. Also the log-normal and Rician distributions may be closely approximated by the Nakagami distribution in some ranges of mean signal values. Nakagami-m distribution is widely used to describe channels with severe to moderate fading. [4] Furthermore, the Nakagami distribution is more flexible and more accurately fit experimental data for many physical propagation channels than the log-normal and Rician distributions.

The entries of the Nakagami-m fading channels are modelled as [4],

$$h_{nrnt} = \sqrt{\sum_{i=1}^{m} |Xi|^2} + j \sqrt{\sum_{i=1}^{m} |Yi|^2} \quad (2.4)$$

where X_i and Y_i are an identical and independently distributed (i.i.d.) Gaussian random variables with μ_X and μ_Y means and σ^2_X and σ^2_Y variances.

The Nakagami-m distribution is parameterized by m and **Ω**. The parameter m is called the 'shape factor. The envelope of the Nakagami-m fading channel is distributed according to Eqn. 2.5 [4],

$$p_v(\vartheta) = \frac{2m^m \vartheta^{2m-1}}{\Gamma(m)} \exp(-m\vartheta^2) \quad (2.5)$$

where $\Gamma(.)$ is the Gamma function.
Furthermore, the pdf of the phase is given by Eqn. 2.6 [4],

$$p_\Theta(\theta) = \frac{\Gamma(m)|\sin(2\theta)|^{m-1}}{2^m \Gamma^2(m/2)} \quad (2.6)$$

From (2.6), the phase of the Nakagami-m fading channel is uniform only when m = 1, where the Nakagami-m fading corresponds to a Rayleigh fading. However, for any m ≠ 1, the phase of the Nakagami-m fading channels is not uniformly distributed.

Another Nakagami-m channel model generally considered in literature models the channel as given in eqn. 2.7 [4],

$$h_{r,t} = \vartheta_{r,t} \exp(j\theta_{r,t}) \quad (2.7)$$

Where ${\vartheta_{r,t}}^2 = \sum_{i=1}^{m} x_i^2 + y_i^2$, with x_i and y_i being i.i.d Gaussian random variables with zero mean and variance of Ω/m. $\vartheta_{r,t}$ can be expressed as a gamma-distributed random variable since it is a sum of 2 squared normal RVs. Here, the phase $\theta_{r,t}$ is a uniform distributed random variable that is independent from $\vartheta_{r,t}$. The distribution of the envelope $\vartheta_{r,t}$is given by [4],

$$p_v(\vartheta) = \frac{2m^m \vartheta^{2m-1}}{\Omega^m \Gamma(m)} \exp(-m\vartheta^2/\Omega) \tag{2.8}$$

Where $\Omega = \mathrm{E}[\vartheta^2]$ and $m = \frac{\mathrm{E}[\vartheta^2]^2}{Var[\vartheta^2]}$. The joint envelope-phase distribution of this Nakagami-m channel model is given by,

$$p_{v,\theta}(\vartheta, \theta) = \frac{m^m \vartheta^{2m-1}}{\pi\Omega^m \Gamma(m)} \exp(-m\vartheta^2/\Omega) \tag{2.9}$$

The PDF of Nakagami-m distribution for different values of m are depicted in Figure 2.3. As can be seen from the figure, when m increases, the Nakagami-m channel approaches Gaussian distribution, which increases the correlation between different channel paths from different transmit antennas [1].

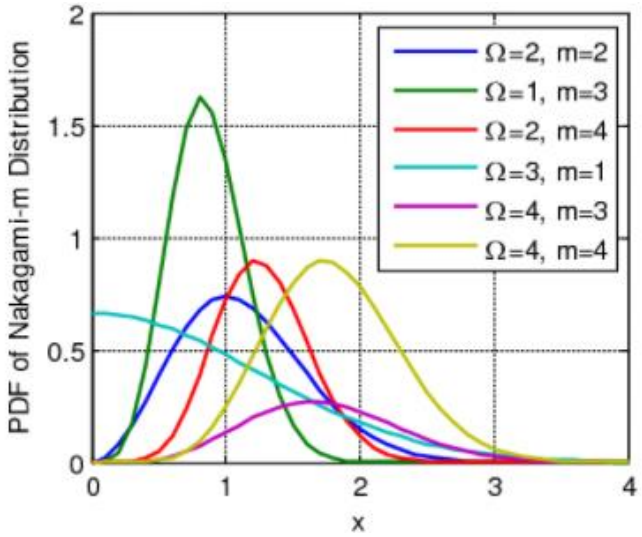

Fig 2.3. PDF of Nakagami-m for various values of m
Source: [5] Huang, Jihua. "Simulation Study of CSI Relay over Nakagami-m Fading Channels." ICIS 2015 (2015).

The extent of fading in the channel is controlled by m which can take values from 0.5 and up, including non-integer values. The value of m is given by the formula, $m = \frac{\mathrm{E}[\vartheta^2]^2}{Var[\vartheta^2]}$. This kind of

distribution is also known as Nakagami-m distribution or chi distribution. The Nakagami-m channel is a generalized fading channel that includes the one-sided Gaussian (m = 1⁄2), the Rayleigh fading (m = 1), and if m → ∞, the Nakagami-m fading channel converges to a nonfading AWGN channel [1]. Furthermore, when m < 1, the Nakagami-m can closely approximate the Nakagami-q (Hoyt) distribution.

2.5. Kronecker correlation model

In order to simulate a spatially correlated channel, the Kronecker correlation model for spatially correlated MIMO systems has been used and is given by [5],

$$H = \Sigma_r^{1/2} \widehat{H}\, \Sigma_t^{1/2} \tag{2.10}$$

where $\sum_r$ and $\sum_t$ are the receive and transmit correlation matrices, respectively, and $\widehat{H}$ is an $N_r \times N_t$ matrix with entries distributed according to the Nakagami-m distribution. $\sum_r$ and $\sum_t$ follow the exponential decay model given by [5],

$$\sum_{rij} = \sum_{tij} = \lambda^{|i-j|} \tag{2.11}$$

where $0 < \lambda < 1$ for both Σr and Σt.

Spatial correlation of one of the channel imperfections that can occur which degrades the performance of the system. There are two factors which determine the channel correlation - the environment and the spacing of the antenna elements. Even if a terminal is surrounded by a lot of scatterers, the correlation can be kept to a low even if the antennas are separated by half a wavelength. In outdoor base stations, however, low correlation is likely to require more than 10 wavelengths between neighbouring antenna elements since the antennas are much higher than the scatterers [1]. In indoor base stations, the required antenna separation is between half and 10 wavelengths. It is assumed here that the correlations at the transmitter and the receiver arrays are independent of each other since the distance between the transmit and receive arrays is large compared to the antenna element spacing [1].

To incorporate the SC into the channel model, the correlation among channels at multiple elements needs to be calculated. The cross correlation φ_{ij}^{Tx} between the channel coefficients of the two antenna elements i and j at the transmitter array can be calculated as [1],

$$\varphi_{ij}^{Tx} = \langle\, |h_i|^2, |h_j|^2 \,\rangle \tag{2.12}$$

where h_i is the channel vector between transmit antenna *i* and all receive antennas, and $\langle \cdot, \cdot \rangle$ is the inner product. In a similar way, the cross correlation φ_{ij}^{Rx} between the two antenna elements *i* and *j* at the receiver array can be computed.

The transmit and receive correlation matrices (R_{Tx} and R_{Rx}) contain information about how signals from each element at the transmitter and receiver are correlated with each other. They are given as [1],

$$R_{T_x} = \begin{bmatrix} \varphi_{11}^{Tx} & \cdots & \varphi_{1N_t}^{Tx} \\ \vdots & \ddots & \vdots \\ \varphi_{N_t1}^{Tx} & \cdots & \varphi_{N_tN_t}^{Tx} \end{bmatrix} \tag{2.13}$$

$$R_{R_x} = \begin{bmatrix} \varphi_{11}^{Rx} & \cdots & \varphi_{1N_r}^{Rx} \\ \vdots & \ddots & \vdots \\ \varphi_{N_r1}^{Rx} & \cdots & \varphi_{N_rN_r}^{Rx} \end{bmatrix} \tag{2.14}$$

The correlated channel matrix is then obtained as,

$$H^{corr} = R_{Rx}^{1/2} H\, R_{Tx}^{1/2} \tag{2.15}$$

Spatial correlation depends on the eigenvalue distribution of the correlation matrices. A high correlation implies a large eigenvalue spread and that some spatial directions give more gain and are statistically stronger than others. Therefore, as m increases, the distribution gets taller and narrower. Smaller eigenvalue spread results in lower signal correlation.

2.6.Antenna Grouping

In practical wireless communication systems, the transmit antennas are placed very close to each other due to space restraints of the wireless terminals. This results in high correlation among the antennas when a large number of antennas are used. This correlation among the transmit antennas

will lead to a situation where the active antenna indices will not be detected accurately. This error will intern influence the detection of the symbols transmitted by these active antennas. Antenna grouping proves to be a technique which can improve the system performance when it is under high channel correlation [6]. This is a way to map the space bits to the indices of active antennas which can weaken the impact of the transmit antenna correlation.

In block grouping, the antennas that are adjacent to each other are divided into different groups [6]. For example, if the number of active antennas is chosen as 2, the antennas are divided into two adjacent groups as shown in figure 2.4. One antenna from each group is chosen to be active. It can be seen here that block grouping method does not significantly help with the channel correlation problem. However, dividing antennas into groups and choosing one active antenna from each group does significantly reduce the detection error rate when there is high channel correlation.

In interleaved grouping, the antennas of each group are distributed in the whole linear array evenly. If 2 antennas are chosen to be active, the antennas will be assigned to 2 groups alternatively as seen in figure 2.4. This maximizes the distance between the active antennas which minimizes the antenna correlation. Interleaved grouping therefore, further improved the performance of a system under channel correlation compared to block coding.

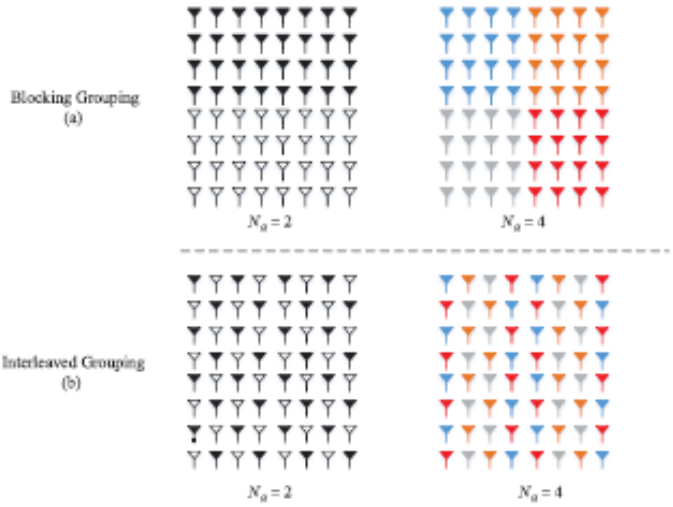

Fig 2.4. Two grouping schemes for 2-dimensional transmit antenna array (Nt = 8 x 8; Na = 2 or 4).
Source: [6] W. Qu, M. Zhang, X. Cheng and P. Ju, "Generalized Spatial Modulation with Transmit Antenna Grouping for Massive MIMO,"

CHAPTER 3
METHODOLOGY

3.1. Introduction

This chapter will hold the methodology used to build the Enhanced Spatial Modulation constellation diagram. This is done using primary and secondary constellation formed using geometric interpolation. The design procedure for ESM will be explained including antenna combinations considered and calculation of bpcu. This design procedure is then used to further generalise ESM to build systems of different configurations.

Further, the Matlab Simulation used to implement ESM systems is discussed highlighting the step-by-step procedure.

3.2. Enhanced Spatial Modulation

In ESM, in addition to adding a third dimension with the antenna array indices, the incoming bits are mapped to geometrically interpolated secondary constellations derived from the primary constellation [2]. Throughout this project, 16QAM has been considered i.e, M=16. Instead of using the original primary constellation P_M, a subset $P_{M/2}$ which consists of the M/2 points of P_M of smallest energy is considered. Since both of the constellations used in this design have the same size and essentially the same average energy, we do not need to restrict here that half of the symbols must take their values from $P_{M/2}$ and the other half from the $S_{M/2}$ constellation. All we need instead is to have an even number of symbols taking their values from $S_{M/2}$, as this condition is sufficient to ensure that the minimum Euclidean distance in the signal space will not be reduced.

For M = 16, it is a (non-conventional) 8QAM signal constellation given by Eqn. 3.1,

$$P_8 = \{\pm 1 \pm i, 3 + i, 1 - 3i, -3 - i, -1 + 3i\} \tag{3.1}$$

And S_8 is given as,

$$S_8 = \{\pm 2 \pm 2i, \pm 2, \pm 2i\} \tag{3.2}$$

This constellation is shown in Fig. 3.1 together with P_8 and S_8.

Here, multiple constellations are used in order to increase the number of code words compared to previously used Spatial Modulation techniques where active antenna indices and primary constellation alone are used. In this design, the minimum Euclidian distance of the primary constellation is maintained. The additional constellations too have a minimum Euclidean distance, but the minimum distance between points selected from different constellations is smaller than this value. This makes a minimum distance of between the points of the primary constellation and those of the secondary constellation derived after the first interpolation step.

In ESM-Type2, the design procedure is as follows: The transmitted code words x belongs to a signal space *L*, which is the union of four subspaces *L1, L2, L3, L4: x ∈{L1, L2, L3, L4}.* The first three subspaces are defined as given in Eqn. 3.3, 3.4 and 3.5 [2],

$$L_1 = \left\{ \begin{bmatrix} P_{M/2} \\ S_{M/2} \\ 0 \\ 0 \end{bmatrix}, \begin{bmatrix} S_{M/2} \\ P_{M/2} \\ 0 \\ 0 \end{bmatrix}, \begin{bmatrix} 0 \\ 0 \\ P_{M/2} \\ S_{M/2} \end{bmatrix}, \begin{bmatrix} 0 \\ 0 \\ S_{M/2} \\ P_{M/2} \end{bmatrix} \right\} \tag{3.3}$$

$$L_2 = \left\{ \begin{bmatrix} P_{M/2} \\ 0 \\ S_{M/2} \\ 0 \end{bmatrix}, \begin{bmatrix} S_{M/2} \\ 0 \\ P_{M/2} \\ 0 \end{bmatrix}, \begin{bmatrix} 0 \\ P_{M/2} \\ 0 \\ S_{M/2} \end{bmatrix}, \begin{bmatrix} 0 \\ S_{M/2} \\ 0 \\ P_{M/2} \end{bmatrix} \right\} \tag{3.4}$$

$$L_3 = \left\{ \begin{bmatrix} P_{M/2} \\ 0 \\ 0 \\ S_{M/2} \end{bmatrix}, \begin{bmatrix} S_{M/2} \\ 0 \\ 0 \\ P_{M/2} \end{bmatrix}, \begin{bmatrix} 0 \\ P_{M/2} \\ S_{M/2} \\ 0 \end{bmatrix}, \begin{bmatrix} 0 \\ S_{M/2} \\ P_{M/2} \\ 0 \end{bmatrix} \right\} \tag{3.5}$$

Different subspaces use different active antenna combinations, but in all of these three subspaces one active antenna transmits symbols from the $P_{M/2}$ signal constellation, while the other active antenna transmits symbols from the $S_{M/2}$ constellation. Note that $2 \log_2 M - 2$ information bits are conveyed by the transmitted symbols, and 2 information bits are used to select one antenna combination in each subspace [2]. Also, 2 prefix bits select a particular L_j subspace, and hence the total number of bits per channel use is $2 + 2 \log_2 M$.

The fourth signal subspace L_4 is more involved. For M = 16, it is given by Eqn. 3.6 [2],

$$L_4 = \left\{ \begin{bmatrix} Q_4 \\ S_8 \\ 0 \\ 0 \end{bmatrix}, \begin{bmatrix} S_8 \\ Q_4 \\ 0 \\ 0 \end{bmatrix}, \begin{bmatrix} 0 \\ 0 \\ Q_4 \\ S_8 \end{bmatrix}, \begin{bmatrix} 0 \\ 0 \\ S_8 \\ Q_4 \end{bmatrix}, \begin{bmatrix} Q_4 \\ 0 \\ S_8 \\ 0 \end{bmatrix}, \begin{bmatrix} S_4 \\ 0 \\ Q_8 \\ 0 \end{bmatrix}, \begin{bmatrix} 0 \\ Q_4 \\ 0 \\ S_8 \end{bmatrix}, \begin{bmatrix} 0 \\ S_8 \\ 0 \\ Q_4 \end{bmatrix} \right\} \quad (3.6)$$

The symbols in signal subspace L_4 carry 5 information bits only, but this subspace includes 8 active antenna and modulation combinations, and therefore 3 bits are needed to select one of them. Together with the prefix bits assigned to the L_4 subspace itself, 10 bits are transmitted per each channel use.

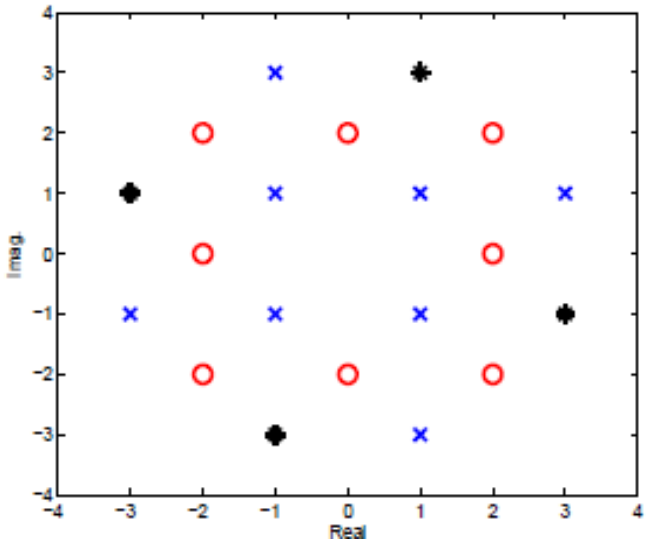

Fig.3.1 The constellations used in ESM with M = 16. The blue crosses represent P8, the red circles represent S8, and the black stars represent Q4.

Source: [2] C. Cheng, H. Sari, S. Sezginer and Y. T. Su, "New signal design for enhanced spatial modulation with multiple constellations,"

This same design procedure for ESM is generalized for various values of N_t, N_r and eta and used to simulated systems of different configurations for different eta values.

For ESM 8x4, where Nt=8, Nr=4, M=16. Here, 3 information bits are used to select one antenna combination in each subspace, 2 prefix bits select a particular Lj subspace 3 bits each for symbol selection from P_8 and S_8.

Therefore, bpcu = 11 which gives 2^{11} possible codeword combinations.

Here, the concepts of antenna grouping are applied in order to improve the performance of the ESM system. First, block grouping is used where adjacent antennas are grouped together.

Since the number of active antennas are chosen to be 2, the antennas are divided into 2 groups in the following way,

Group 1: Antennas 1, 2, 3, 4
Group 2: Antennas 5, 6, 7, 8
One antenna is chosen to be active from each group.

The four subspaces are defined using block grouping as,

$$L_1 = \left\{ \begin{bmatrix} P_8 \\ 0 \\ 0 \\ 0 \\ S_8 \\ 0 \\ 0 \\ 0 \end{bmatrix}, \begin{bmatrix} 0 \\ P_8 \\ 0 \\ 0 \\ S_8 \\ 0 \\ 0 \\ 0 \end{bmatrix}, \begin{bmatrix} 0 \\ 0 \\ P_8 \\ 0 \\ S_8 \\ 0 \\ 0 \\ 0 \end{bmatrix}, \begin{bmatrix} 0 \\ 0 \\ 0 \\ P_8 \\ 0 \\ 0 \\ 0 \\ S_8 \end{bmatrix}, \begin{bmatrix} S_8 \\ 0 \\ 0 \\ 0 \\ P_8 \\ 0 \\ 0 \\ 0 \end{bmatrix}, \begin{bmatrix} 0 \\ S_8 \\ 0 \\ 0 \\ P_8 \\ 0 \\ 0 \\ 0 \end{bmatrix}, \begin{bmatrix} 0 \\ 0 \\ S_8 \\ 0 \\ P_8 \\ 0 \\ 0 \\ 0 \end{bmatrix}, \begin{bmatrix} 0 \\ 0 \\ 0 \\ S_8 \\ 0 \\ 0 \\ 0 \\ P_8 \end{bmatrix} \right\} \tag{3.7}$$

$$L_2 = \left\{ \begin{bmatrix} P_8 \\ 0 \\ 0 \\ 0 \\ 0 \\ S_8 \\ 0 \\ 0 \end{bmatrix}, \begin{bmatrix} 0 \\ P_8 \\ 0 \\ 0 \\ 0 \\ S_8 \\ 0 \\ 0 \end{bmatrix}, \begin{bmatrix} 0 \\ 0 \\ P_8 \\ 0 \\ 0 \\ S_8 \\ 0 \\ 0 \end{bmatrix}, \begin{bmatrix} 0 \\ 0 \\ 0 \\ P_8 \\ 0 \\ S_8 \\ 0 \\ 0 \end{bmatrix}, \begin{bmatrix} S_8 \\ 0 \\ 0 \\ 0 \\ 0 \\ P_8 \\ 0 \\ 0 \end{bmatrix}, \begin{bmatrix} 0 \\ S_8 \\ 0 \\ 0 \\ 0 \\ P_8 \\ 0 \\ 0 \end{bmatrix}, \begin{bmatrix} 0 \\ 0 \\ S_8 \\ 0 \\ 0 \\ P_8 \\ 0 \\ 0 \end{bmatrix}, \begin{bmatrix} 0 \\ 0 \\ 0 \\ S_8 \\ 0 \\ P_8 \\ 0 \\ 0 \end{bmatrix} \right\} \tag{3.8}$$

$$L_3 = \left\{ \begin{bmatrix} P_8 \\ 0 \\ 0 \\ 0 \\ 0 \\ 0 \\ S_8 \\ 0 \end{bmatrix}, \begin{bmatrix} 0 \\ P_8 \\ 0 \\ 0 \\ 0 \\ 0 \\ S_8 \\ 0 \end{bmatrix}, \begin{bmatrix} 0 \\ 0 \\ P_8 \\ 0 \\ 0 \\ 0 \\ S_8 \\ 0 \end{bmatrix}, \begin{bmatrix} 0 \\ 0 \\ 0 \\ P_8 \\ 0 \\ 0 \\ S_8 \\ 0 \end{bmatrix}, \begin{bmatrix} S_8 \\ 0 \\ 0 \\ 0 \\ 0 \\ 0 \\ P_8 \\ 0 \end{bmatrix}, \begin{bmatrix} 0 \\ S_8 \\ 0 \\ 0 \\ 0 \\ 0 \\ P_8 \\ 0 \end{bmatrix}, \begin{bmatrix} 0 \\ 0 \\ S_8 \\ 0 \\ 0 \\ 0 \\ P_8 \\ 0 \end{bmatrix}, \begin{bmatrix} 0 \\ 0 \\ 0 \\ S_8 \\ 0 \\ 0 \\ P_8 \\ 0 \end{bmatrix} \right\} \tag{3.9}$$

$$L_4 = \left\{ \begin{bmatrix} Q_8 \\ 0 \\ 0 \\ 0 \\ S_8 \\ 0 \\ 0 \\ 0 \end{bmatrix} \begin{bmatrix} 0 \\ Q_8 \\ 0 \\ 0 \\ S_8 \\ 0 \\ 0 \\ 0 \end{bmatrix} \begin{bmatrix} 0 \\ 0 \\ Q_8 \\ 0 \\ S_8 \\ 0 \\ 0 \\ 0 \end{bmatrix} \begin{bmatrix} 0 \\ 0 \\ 0 \\ Q_8 \\ 0 \\ 0 \\ 0 \\ S_8 \end{bmatrix} \begin{bmatrix} Q_8 \\ 0 \\ 0 \\ 0 \\ S_8 \\ 0 \\ 0 \\ 0 \end{bmatrix}, \begin{bmatrix} 0 \\ Q_8 \\ 0 \\ 0 \\ S_8 \\ 0 \\ 0 \\ 0 \end{bmatrix}, \begin{bmatrix} 0 \\ 0 \\ Q_8 \\ 0 \\ S_8 \\ 0 \\ 0 \\ 0 \end{bmatrix}, \begin{bmatrix} 0 \\ 0 \\ 0 \\ Q_8 \\ 0 \\ S_8 \\ 0 \\ 0 \end{bmatrix}, \begin{bmatrix} S_8 \\ 0 \\ 0 \\ 0 \\ Q_8 \\ 0 \\ 0 \\ 0 \end{bmatrix}, \begin{bmatrix} 0 \\ S_8 \\ 0 \\ 0 \\ Q_8 \\ 0 \\ 0 \\ 0 \end{bmatrix}, \begin{bmatrix} 0 \\ 0 \\ S_8 \\ 0 \\ Q_8 \\ 0 \\ 0 \\ 0 \end{bmatrix}, \begin{bmatrix} 0 \\ 0 \\ 0 \\ S_8 \\ Q_8 \\ 0 \\ 0 \\ 0 \end{bmatrix}, \begin{bmatrix} S_8 \\ 0 \\ 0 \\ 0 \\ 0 \\ Q_8 \\ 0 \\ 0 \end{bmatrix}, \begin{bmatrix} 0 \\ S_8 \\ 0 \\ 0 \\ 0 \\ Q_8 \\ 0 \\ 0 \end{bmatrix}, \begin{bmatrix} 0 \\ 0 \\ S_8 \\ 0 \\ 0 \\ Q_8 \\ 0 \\ 0 \end{bmatrix}, \begin{bmatrix} 0 \\ 0 \\ 0 \\ S_8 \\ 0 \\ Q_8 \\ 0 \\ 0 \end{bmatrix} \right\} \tag{3.10}$$

Similarly, 8x4 ESM can also be implemented using interleaved grouping where the antennas are grouped into 2 groups alternatively. In this case the groups are,
G1: 1, 3, 5, 7
G2: 2, 4, 6, 8

In interleaved grouping, the average distance between the antennas is maintained and is maximized to minimize the channel correlation.

Here, each of the four subspaces have 512 possible combinations of bits. A block of 11 user bits is mapped to a constellation/symbol/antenna index according to 8x4 ESM mapping. The transmitted symbols are sent over a correlated Nakagami fading channel. Simulations were carried out for this 8x4 ESM scheme with m = 1, 2 and 3.

Similarly, 16x4 is implemented using the above concepts. Both block and interleaved grouping has been carried out with all the 16 antennas divided into 2 groups with one antenna from each group active. In this case, for N_t=16, N_r=4, M=16, 4 information bits are used to select one antenna combination in each subspace. 2 prefix bits select a particular L_j subspace, 3 bits each for symbol selection from P_8 and S_8. Therefore, bpcu = 12. 2^{12} possible codeword combinations.

The two groups for block grouping are,
Group 1: Antennas 1, 2, 3, 4, 5, 6, 7, 8
Group 2: Antennas 9, 10, 11 ,12 ,13, 14, 15, 16

This results in the following subspaces with the mentioned antenna combinations,
L1 = {[1, 9], [2, 9], [3, 9], [4, 9], [5, 9], [6, 9], [7, 9], [8, 9]}
L2 = {[1, 10], [2, 10], [3, 10], [4, 10], [5, 10], [6, 10], [7, 10], [8, 10]}
L3 = {[1, 11], [2, 11], [3, 11], [4, 11], [5, 11], [6, 11], [7, 11], [8, 11]}
L4 = {[1, 9], [2, 9], [3, 9], [4, 9], [5, 9], [6, 9], [7, 9], [8, 9], [1, 10], [2, 10], [3, 10], [4, 10], [5, 10], [6, 10], [7, 10], [8, 10]}

3.3. Methodology

In the simulation process, the goal was to reach a symbol error rate (SER) of at least 10^{-4} to evaluate the performances of the systems. Therefore, for each Eb/ No, at least 1,00,000 information

bits were simulated for each system. One run of sending about 1,00,000 bits for all Eb/ No values is called a Monte Carlo run. The systems were simulated for a specified number of Monte Carlo runs and the results were averaged such that the SER curves were smooth enough for evaluation.

MATLAB Simulation

• Step 1 – The ESM constellation diagram is formed using the design procedure for ESM explained in section 3.2.

• Step 2 – A random sequence of 0's and 1's is generated.

• Step 3 – The generated bits are mapped to a constellation/symbol/antenna index according to ESM mapping.

• Step 4 – The $\widehat{H}$-matrix is generated for Nakagami-m fading channel, with the varying fade parameter 'm'.

• Step 5 – Correlation matrices $\sum_r$ and $\sum_t$ are computed using exponential decay model (Eqn. 2.11).

• Step 6 – The final H for spatially correlated channel is computed using eqn. 2.10.

• Step 7 – The signal at the receiver is obtained by multiplying the modulated data with the H-matrix of the channel and an additive white Gaussian noise is added to the transmitted data.

• Step 8 – At the receiver, joint detection of the combination bits and constellation bits takes place through the optimal maximum likelihood (ML) detection. The received signal is compared to the original transmitted signal to count the number of bit errors.

• Step 9 – SER is computed and simulated.

• Step 10 – The procedure is repeated for varying values of the Nakagami m parameter to simulate the SER results under different fading channel conditions in indoor environments. The value of 'm' is varied between m=1 and m=3

• Step 11 – The obtained symbol error rate was used to compare the respective performances of conventional SM schemes and ESM.

In all depicted result plots, the E_b/N_o, is depicted versus symbol error ratio using the 'semilogy' function in Matlab.

3.4. Conclusion

Using the methodology described in this chapter, results from the various simulations are found. This includes the SER vs E_b/N_o performance of 4x4, 8x4 and 16x4 ESM under correlated Nakagami-m with different values of m and an analysis for 4x4 ESM under Nakagami-m and the η-μ fading channel models with non-uniform phase, and with uniform phase distributions. In addition, the performance of ESM with SM and GSM for 4x4 and 8x4 is also carried out.

CHAPTER 4
CASE STUDY: HIGH ALTITUDE PLATFORMS

Due to the increasing demand of wireless services, it has become crucial to find was to make access of wireless services easier and expand internet access to areas that could not be reached by wired technology. There is a demand to find cost effective reliable and novel ways to deliver wireless services for next generation multimedia applications. A possible way to do this is using high altitude platforms (HAPs). HAPs are planes or airships that float through the stratosphere about 20 km above the ground [7]. These platforms have the capability to cater to a large number of users with considerably less communication infrastructure that a terrestrial network would require.

The highlight of HAPs is that there are nearer to the earth than satellites but still high enough to maintain a wide area coverage. This gives it the ability to reduce latency as well as exhibit the promising features of both terrestrial and satellite networks. Adding to this, HAPs are considered environmental friendly, cost effective and flexible as compared to the terrestrial and satellite systems [7].

A main advantage of using HAP is that a much stronger signal is received from HAP compared to the one from a satellite. This would cause a reduction in the transmission power and would decrease the size of the repeater used in HAP. HAPs are also easier to deploy such that a high speed connection can be obtained over a sizeable geographic area. The main aim of HAPs is to provide a lasting data rate, high capacity and density capability over a wide coverage area from a fixed point in the sky. One of the main reasons why HAPS-based communication systems are highly favored is because they prove to have free-space like path loss characteristics. Another benefit of using HAPs is that there is a shorter delay for a signal travelling from the HAP to the ground compared to that from a satellite.

The traditional MIMO method in HAP has a channel of mainly LOS channel, weak spread, directional antennas and small size of platforms. This makes it very accessible. However, a virtual MIMO system can be formed by placing many platforms in any arrangement and organize inter-platform links such that the platforms can communicate with a multi-antenna system on the ground. One application of this is on fast moving trains where this multi-antenna system can be placed on these trains and connect to multiple HAPs which provide steady broadband wireless access under LOS propagation surroundings [7]. With the effect of shadowing of these platforms

due to the environment these trains operate in, the channels of individual HAPs are statistically independent which gives diversity multiplexing gain. While inter platform links do increase the complexity of the payload, it increases the capacity, reduce system requirements in the ground segment by providing support above the ground and improve coverage area. They are only limited by power and processing constraints. In Figure 4.1., a 3x2 MIMO channel is formed based on this idea.

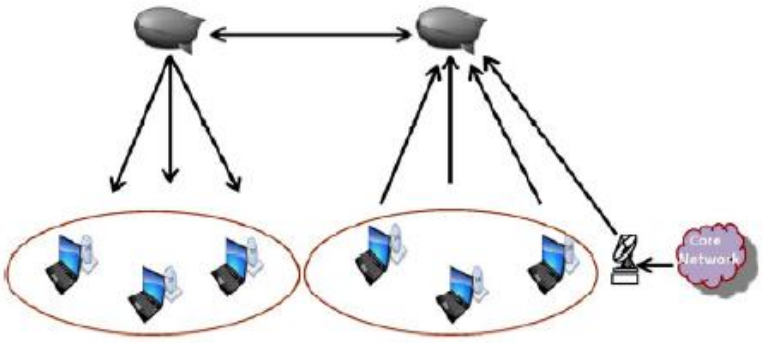

Fig 4.1. A constellation of multiple interconnected HAPs
Source: MIMO Channel Modeling for Integrated High Altitude Platforms, Geostationary Satellite/Land Mobile Satellite and Wireless Terrestrial Networks, Aamir Habib and Qamar-ul-Islam

There is however a problem in that the mobile users are usually not evenly distributed in the coverage area. Sometimes, the users aggregate around hotspots like a fire or crime scene or an earthquake center. These areas require high speed connections and are densely packed. Usually HAPs consists of directional antennas which produce circular spot beams on the ground with a radius of several kilometers. The size of this beam is usually bigger than the hotspot and therefore the hotspot is served by only one beam. This limits the hotspot's capacity since there can be no spatial multiplexing gain. In addition to this, the hotspot capacity is further reduced due to the inter-beam interference caused by the side lobe effect of the directional antenna. One way around solving this problem can be the method described above by using a virtual MIMO system where platforms can connect to multi antenna systems on the ground and make use of the spatial multiplexing gain that MIMO provides.

There is another way that MIMO systems can be incorporated into HAPs to impart its benefits to the system. To overcome problems like deteriorated performance for users at the edge coverage since at low elevation there is a huge fading depth, MIMO can be employed. MIMO which allows for diversity and spatial multiplexing gain can improve the bad performance at low elevation platforms. In this case, MIMO can be implemented on a single HAP with sufficient spacing depending on the frequency. HAPs is then a transmitter with multiple antennas with multiple

receiver antennas on the ground [7]. This will be really helpful in order to handle the severe fading between the transmitter and receiver at low elevation angles and improve the BER. In order to increase the capacity, MIMO techniques such as Spatial Multiplexing and Spatial Modulation can be used. HAP based communication combined with MIMO can achieve multiplexing gain thus increase the capacity and improve spectral efficiency at the hotspots. The concepts of Enhanced Spatial Modulation implemented in this project can be applied to the MIMO-HAP combined system in order to further improve the performance and spectral efficiency. This could be an efficient solution to overcome the problems that HAPs face in proving high speed communication to the users in densely packed hotspots and overcoming severe fading effects caused at the edge of the coverage in HAPs.

CHAPTER 5
RESULT ANALYSIS

5.1. Introduction

In this chapter, the results from the various simulations carried out will be presented. The plots of SER vs E_b/N_o performance of 4x4, 8x4 and 16x4 ESM under correlated Nakagami-m with different values of m will be seen. This chapter will also include an analysis for 4x4 ESM under Nakagami-m with non-uniform phase, and with uniform phase distributions. Finally, the plots comparing the performance of ESM with SM and GSM for 4x4, 8x4 and 16x4 shall be observed and discussed.

5.2. Result Analysis

Monte Carlo simulations were carried out using uncorrelated Nakagami-m fading MIMO channels and assuming perfect CSI at the receiver. In the simulations, symbol code words X were randomly generated transmitted over the channel, the decoding was performed using the received noisy signal samples, and error events $X \neq X'$ were counted. The obtained symbol error rate (SER) was plotted with the E_b/N_o. In Monte-Carlo simulation results, at least 10^5 bits are simulated for each E_b/N_o value. All the simulations were carried out using Matlab 2019.

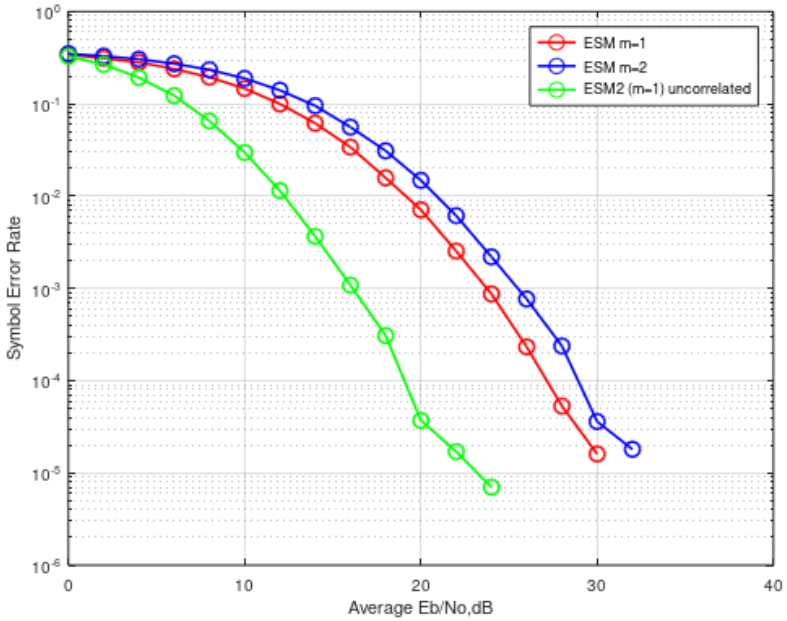

Fig 5.1. SER vs E_b/N_o performance for ESM 4x4 under Nakagami channel for various m values, 10 bpcu

Figure 5.1. shows the performance of ESM 4x4 for correlated Nakagami-m with m = 1 and m = 2 and uncorrelated Nakagami-m with m = 1 where λ was taken to be 0.8. It can be seen that as m increases, the SER for a particular E_b/N_o also increases. This is because, as m increases, the distribution gets taller and narrower. Smaller eigenvalue spread results in lower signal correlation. Lower signal correlation gives lesser symbol error rate. Uncorrelated Nakagami-m channel as expected, experiences less performance degradation.

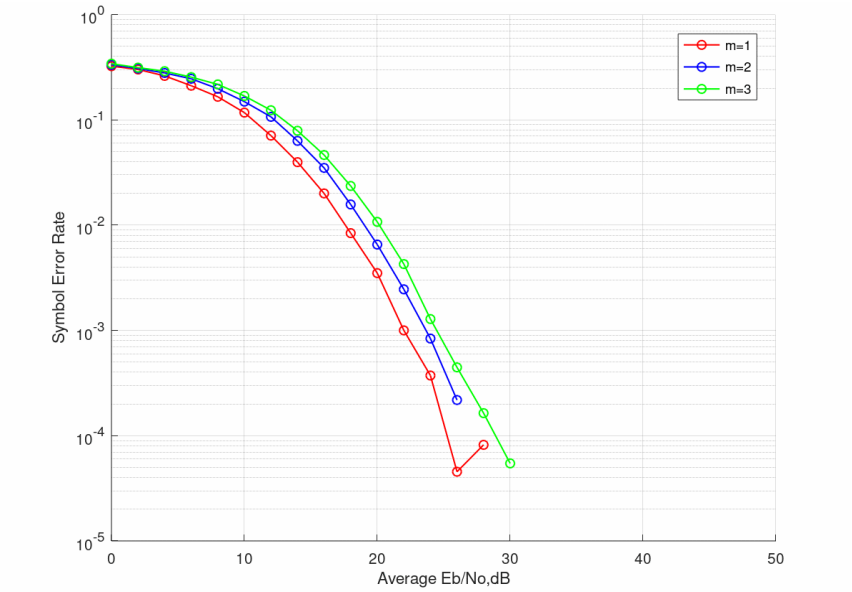

Fig 5.2. SER vs E_b/N_o performance for ESM 8x4 with block grouping under Nakagami channel for m = 1, 2, 3

Figure 5.2. shows the performance of ESM 8x4 with block grouping for correlated Nakagami-m with m = 1,2,3 where λ was taken to be 0.8. Similar to ESM 4x4, the SER for a particular E_b/N_o increases as m increases due to the reasons explained earlier.
It can be seen that a good system performance can be achieved with the ESM 4x4 and 8x4 scheme (≈ 25-28 dB E_b/N_o for 10^{-4} SER).

Figure 5.3. shows the performance of ESM 8x4 for interleaved grouping under correlated Nakagami-m with m = 1,2,3 where λ was taken to be 0.8.

Studies usually assume the Nakagami-m fading channels with a uniform distribution, however, it has been shown that the Nakagami-m channel phase distribution is not uniform. Figure 5.4 and 5.5 are plotted to find out how significantly the channel phase distribution affects the performance of ESM MIMO systems.

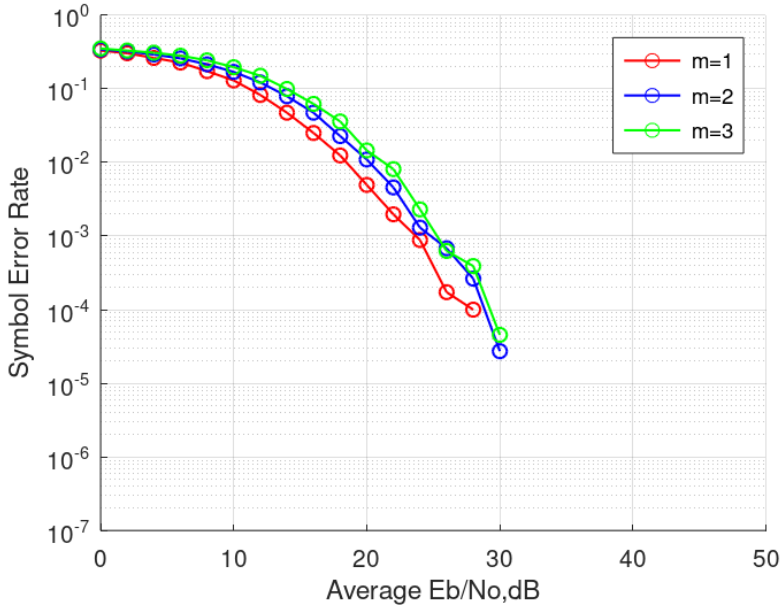

Fig 5.3. SER vs Eb/No performance for ESM 8x4 with interleaved grouping under Nakagami channel m= 1, 2, 3

In this study, a 4 x 4 ESM MIMO system with 16-QAM modulation is considered. Hence, a spectral efficiency of 10 bps/Hz is achieved. The channel state information is assumed to be perfectly known at the receiver side. The Nakagami-m channel models with non-uniform phase, as in eqn. 2.4, and with uniform phase distributions are considered. The SER performance of 4 x 4 ESM MIMO system with 16-QAM modulation versus E_b/N_o over uniform phase correlated Nakagami-m channel modeled as in 2.5, for m = 1; 2; 3 is shown in Figure 5.4. Figure 5.5. shows the performance over non-uniform phase correlated Nakagami-m channel modeled as in 2.5.

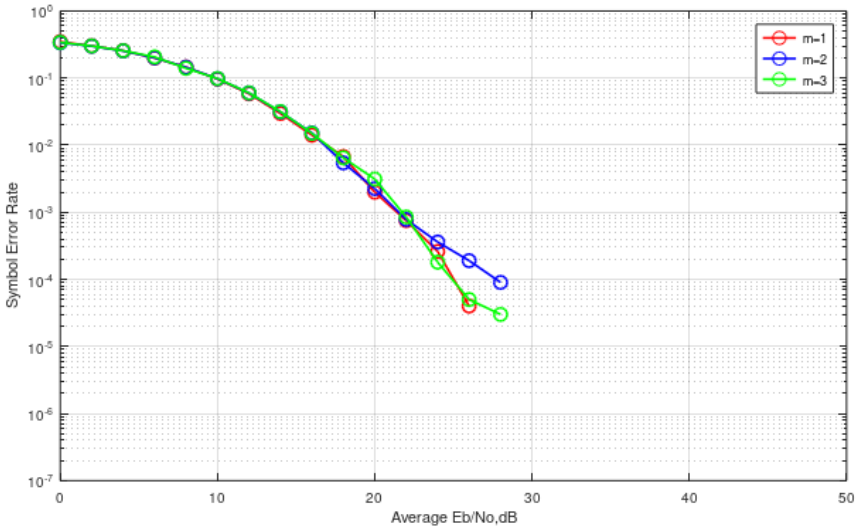

Fig 5.4. SER performance of 4 x 4 ESM MIMO system with 16-QAM modulation versus Eb/No over uniform phase correlated Nakagami-m, 10 bpcu

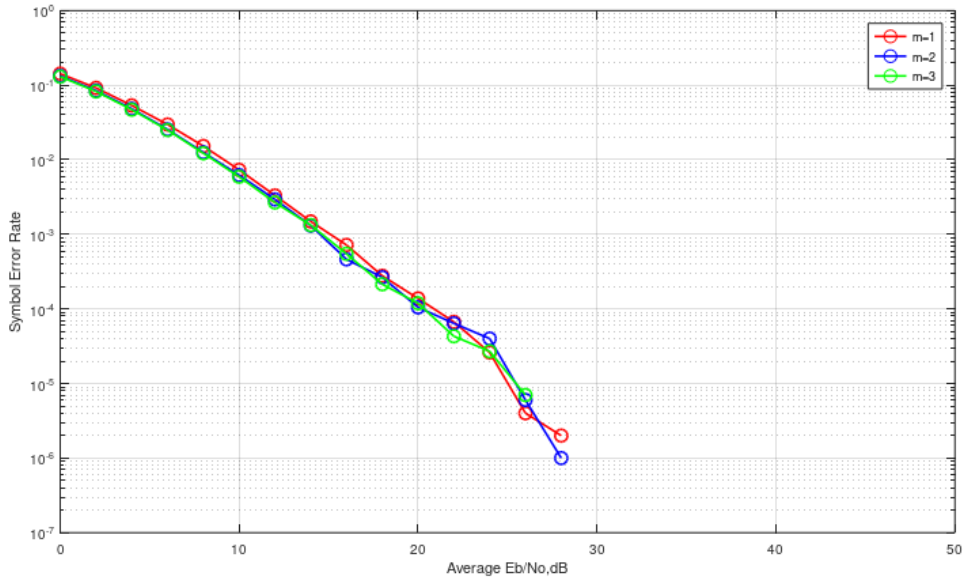

Fig 5.5. SER performance of 4 x 4 ESM MIMO system with 16-QAM modulation versus Eb/No over non-uniform phase correlated Nakagami-m channel modeled as in (2) and for m = 1; 2; 3.

Results for non-uniform phase distribution is different than previously reported uniform phase distribution results, which highlights the significant impact of the channel phase distribution on the performance of ESM MIMO system. It is also shown that increasing the m parameter degrades the performance of the system. It is important to note that as m becomes infinity, the Nakagami-m channel becomes Gaussian and resolving transmitted data from different transmit antennas would be impossible.

It can be seen that Nakagami-m channel with m=2 performs 8 dB worse at 10^{-4} SER when assuming uniform phase distribution as compared to the non-uniform phase distribution. It is shown that wrong results and conclusions are achieved with the assumption of uniform phase distribution for Nakagami-m, therefore, the uniform phase assumption for Nakagami-m fading channel cannot always be assumed.

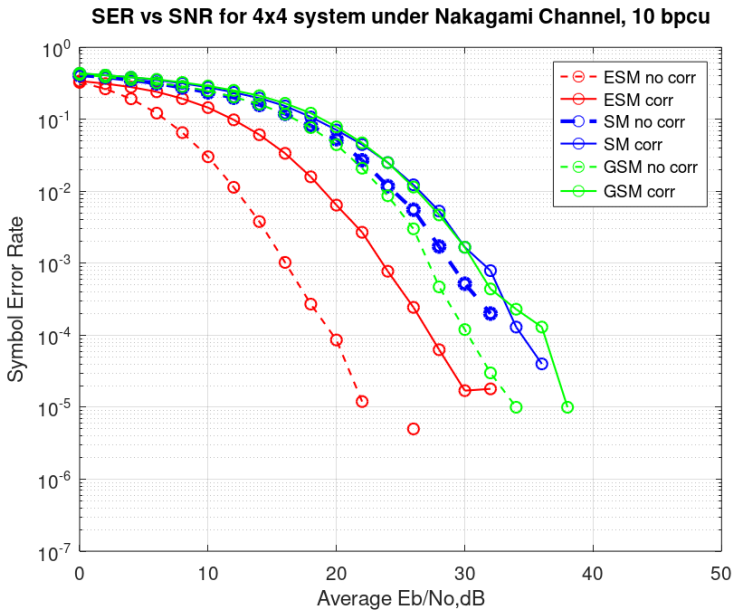

Fig 5.6. SER performance of 4 x 4 ESM, SM and GSM MIMO systems versus Eb/No over Nakagami-m channel

Figure 5.6 shows the performance of ESM, SM and GSM systems over correlated and uncorrelated Nakagami-m fading channel. The dotted lines represent the performances of the three systems over uncorrelated Nakagami-m and the solid lines represent the performances over correlated Nakagami-m for m=1. The bpcu for all the three systems is 10. The system configurations are chosen as given in Table 5.1. The modulation schemes used are 16QAM for ESM, 256QAM for both SM and GSM.

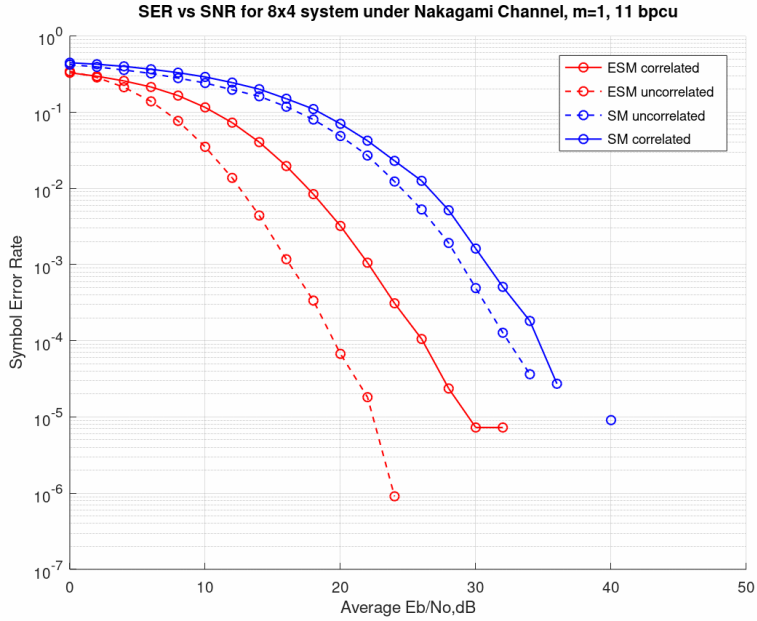

Fig 5.7. SER performance of 8 x 4 ESM, SM and GSM MIMO systems versus Eb/No over Nakagami-m channel

Figure 5.7 shows the performance of ESM, SM and GSM systems over correlated and uncorrelated Nakagami-m fading channel. Similar to the previous plot, the dotted lines represent the performances of the three systems over uncorrelated Nakagami-m and the solid lines represent the performances over correlated Nakagami-m for m=1. The bpcu for all the three systems is 11. The system configurations are chosen as given in Table 5.2. The modulation schemes used are 16QAM for ESM and 256QAM for SM.

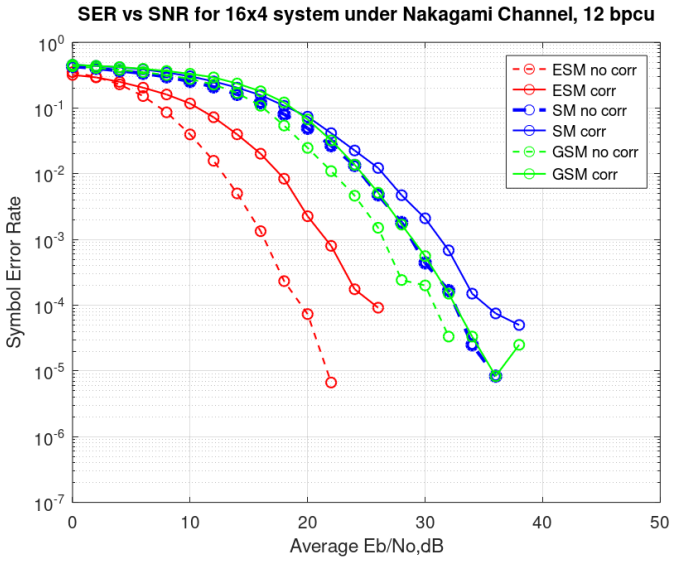

Fig 5.8. SER performance of 16 x 4 ESM, SM and GSM MIMO systems versus Eb/No over Nakagami-m channel

Figure 5.8 shows the performance of ESM, SM and GSM systems over correlated and uncorrelated Nakagami-m fading channel for 16x4.

These plots show that ESM outperforms both SM and GSM in both cases of 4x4, 8x4, 16x4 under correlated Nakagami-m channel. ESM even under correlated Nakagami-m channel (lambda = 0.8) gives a better performance than SM and GSM under uncorrelated Nakagami-m channel. This shows that even the worst possible performance of ESM is better than the best performance of SM and ESM. Therefore, ESM provides a significant performance gain with respect to conventional Spatial Modulation schemes.

5.3. Final Results

All schemes have been evaluated at the same spectral efficiency. We consider that all 4×4 systems are operating at 10 bits/channel use while 8×4 systems are operating at 11 bits/channel use. Table 5.1 and 5.2 summarize these configurations. The 16-QAM based constellation for ESM is shown in Figure 3.1.

Table 5.1. System configuration of 4x4 MIMO, 10bpcu

Scheme	Bits per antenna combination	Bits per constellation symbol	M
ESM	6	4	16
GSM, 2 active antennas	2	8	256
SM	2	8	256

Table 5.2. System configuration of 8x4 MIMO, 11bpcu

Scheme	Bits per antenna combination	Bits per constellation symbol	M
ESM	7	4	16
SM	3	8	256

For 10 bpcu, at BER = 10^{-3}, under the case of Nakagami-m channel with no correlation, ESM has a 13 dB gain over SM and a 11.14 Db gain over GSM. For channel under correlation, at BER = 10^{-3}, ESM has a 7.86 dB gain over SM and a 7.14 dB gain over GSM.
Similarly, at BER = 10^{-4}, under the case of Nakagami-m channel with no correlation, ESM has a 13.3 dB gain over SM and a 10.5 dB gain over GSM. For channel under correlation, at BER = 10^{-4}, ESM has a 7.1 dB gain over SM and an 8.87 dB gain over GSM.

Table 5.3 shows the required E_b/N_o to achieve various SERs. It can be seen that ESM outperforms other conventional spatial modulations.

Table 5.3. E_b/N_o (in dB) to achieve various SERs at 10bpcu

SER	10^{-3}	10^{-4}
ESM uncorrelated	16	19.798
ESM correlated	23.589	27.339
SM uncorrelated	28.992	33.105
SM correlated	31.452	34.435
GSM uncorrelated	27.137	30.282
GSM correlated	30.726	36.21

It is interesting to note that ESM even under correlated Nakagami-m channel outperforms SM and GSM under no correlation by a wide margin with ESM giving around 5.4 dB gain over SM and 3.5 dB gain over GSM at 10^{-3} BER. This shows that even the worst possible performance of ESM is still much better than the best performances of SM and GSM.

In addition, to achieve the same bpcu as ESM, SM and GSM need to employ a very high order modulation scheme according to Table 5.1 and Table. 5.2, which leads to high bit error rates.

Table 5.4. E_b/N_o (in dB) to achieve various SERs at 11bpcu

SER	10^{-3}	10^{-4}
ESM uncorrelated	16.267	19.526
ESM correlated	22.029	25.949
SM uncorrelated	28.925	32.42
SM correlated	30.814	34.639

Table 5.4. gives the E_b/N_o to achieve various SERs at 11bpcu. These results show that at SER = 10^{-3} the presented ESM schemes achieve E_b/N_o gains over SM of around 12.658 dB under uncorrelated channels and 8.785 dB for correlated channels. Note that the gains are higher than those achieved in the 10 bpcu case. This is due to the fact that the average energy of the secondary constellations used in our signal design becomes lower (relatively to the primary constellation) when higher spectral efficiencies are considered.

CHAPTER 6
CONCLUSION AND FUTURE SCOPE OF WORK

6.1.Summary of the work done

The goal of this project was to evaluate the Symbol Error Rate (SER) vs E_b/N_o performances of ESM systems of different configurations with varying spectral efficiencies under correlated Nakagami-m fading. This goal was accomplished by build the ESM system, ESM constellation designs using geometric interpolation are implemented.

The incoming bits are then mapped to a constellation/ antenna index according to ESM mapping. The transmitted symbols are sent over a correlated Nakagami-m fading channel using the Kronecher correlation model for spatially correlated MIMO systems. SER vs E_b/N_o of this system is plotted and analysed for different m values. Further, various SM schemes is looked at to study their performance compared to ESM under the same fading channels.

A comprehensive background of the MIMO systems and Spatial Modulation was presented. The detailed methodogy of ESM and the procedure for simulations was explained. This was used to study the SER vs E_b/N_o performance of 4x4, 8x4 and 16x4 ESM under correlated Nakagami-m with different values of m using antenna grouping. Further, analyse 4x4 ESM under Nakagami-m fading channel models with non-uniform phase, and with uniform phase distributions. Finally, comparison of the performance of ESM with SM and GSM for 4x4, 8x4, 16x4 is observed and discussed.

6.2.Significant Results and Conclusions

The emerging market of the IoT requires novel power-efficient and low-complexity MIMO aided cellular radio access technologies. This trend will have a profound impact on both the theory and practice of future cellular networks, which will no longer be purely optimized for approaching the attainable capacity, but will explicitly include the energy efficiency during the design and optimization of the entire protocol stack. In this project, we have seen that SM constitutes a promising transmission concept in the context of MIMO-aided transmission.

The most significant result of this study was the observation that ESM provides a significant performance gain with respect to conventional Spatial Modulation schemes. These plots show that

ESM outperforms both SM and GSM in both cases of 4x4 and 8x4 under correlated Nakagami-m channel. ESM even under correlated Nakagami-m channel (lambda = 0.8) gives a better performance than SM and GSM under uncorrelated Nakagami-m channel. This shows that even the worst possible performance of ESM is better than the best performance of SM and ESM. Therefore, ESM provides a significant performance gain with respect to conventional Spatial Modulation schemes. at BER = 10^{-4}, under the case of Nakagami-m channel with no correlation, ESM has a 13.3 dB gain over SM and a 10.5 dB gain over GSM. For channel under correlation, at BER = 10^{-4}, ESM has a 7.1 dB gain over SM and an 8.87 dB gain over GSM.

The results for the ESM system under correlated Nakagami-m fading channel indicated that an increase in the shape factor m resulted in lower signal correlation gives lesser symbol error rate. It was also seen that uncorrelated Nakagami-m channel experiences less performance degradation. It was also seen that employing antenna grouping methods significantly improved the performance of the system. It was noted that interleaved grouping proved to be most effective in doing so.

The other significant result was that the assumption of the channel phase distribution showed to significantly affect the performance of ESM MIMO systems. Existing literature assume simplified phase distribution to simplify the derivation of the performance analysis and allow for mathematical tractability. However, it was seen that the assumption of the channel phase distribution has a major impact on the performance and that it is shown that uniform assumption of channel phase distribution is incorrect and leads to erroneous conclusions.

In conclusion, the work was a thorough study on ESM MIMO systems that helped highlight the advantages of ESM techniques under a generalized fading channel i.e. the Nakagami-m fading channel.

6.3.Future Work

The ESM scheme used in this project can be taken one step further by using two additional constellations that are derived through a second interpolation step. The system can be extended by stacking two consecutive received signal vectors and defining the codewords over two consecutive channels.

The ESM system used in this project can be extended to be used in Massive MIMO with a large number of base station antennas to enhance spectral efficiency.

The application MIMO ESM in High Altitude Platforms can be further explored.

REFERENCES

[1] Space modulation techniques by Raed Mesleh, Abdelhamid Alhassi, 2018 JohnWiley & Sons, Inc.

[2] C. Cheng, H. Sari, S. Sezginer and Y. T. Su, "New signal design for enhanced spatial modulation with multiple constellations," 2015 IEEE 26th Annual International Symposium on Personal, Indoor, and Mobile Radio Communications (PIMRC), Hong Kong, 2015, pp. 872-876, doi: 10.1109/PIMRC.2015.7343420.

[3] Marco Renzo, Harald Haas, Ali Ghrayeb, Lajos Hanzo, Shinya Sugiura. Spatial Modulation for Multiple-Antenna Communication. John G. Webster. Wiley Encyclopedia of Electrical and Electronics Engineering, 2016, ff10.1002/047134608X.W8327ff. ffhal-02324436f

[4] Mesleh, R., Badarneh, O.S., Younis, A. et al. How significant is the assumption of the uniform channel phase distribution on the performance of spatial multiplexing MIMO system? Wireless Netw 23, 2281–2288 (2017).

[5] A. B. Saleem and S. A. Hassan, "On the Performance of Spatial Modulation Schemes in Large-Scale MIMO under Correlated Nakagami Fading," 2020 IEEE 91st Vehicular Technology Conference (VTC2020-Spring), Antwerp, Belgium, 2020, pp. 1-5, doi: 10.1109/VTC2020-Spring48590.2020.9128726.

[6] W. Qu, M. Zhang, X. Cheng and P. Ju, "Generalized Spatial Modulation With Transmit Antenna Grouping for Massive MIMO," in IEEE Access, vol. 5, pp. 26798-26807, 2017, doi: 10.1109/ACCESS.2017.2775281.

[7] MIMO channel modeling for integrated high altitude platforms, geostationary satellite/land mobile satellite and wireless terrestrial networks. J Aamir HabibQamar Ul Islam, 2013, Journal of Space Technology

[8] G. D. Goutham Simha, S. Koila, R. Mans and U. Sripati, "Modified signal design for multistream spatial modulation over spatially correlated channels," 2017 International Conference on Advances in Computing, Communications and Informatics (ICACCI), 2017, pp. 612-617, doi: 10.1109/ICACCI.2017.8125908.

[9] Goutham Simha G.D., S. Koila, Neha N and U. Sripati, "Performance of Spatial-Modulation and spatial-multiplexing systems over Weibull fading channel," 2015 International Conference on Computing and Network Communications (CoCoNet), 2015, pp. 389-394, doi: 10.1109/CoCoNet.2015.7411215.

[10] G. S. Shrutkirthi, S. G. D. Goutham and U. S. Acharya, "A MIMO SM-NSTBC Scheme for High Altitude Platform Communication Systems: Study and Analysis," 2019 6th International Conference on Signal Processing and Integrated Networks (SPIN), 2019, pp. 53-58, doi: 10.1109/SPIN.2019.8711723.

[11] K. Kim, J. Lee and H. Liu, "Spatial-Correlation-Based Antenna Grouping for MIMO Systems," in IEEE Transactions on Vehicular Technology, vol. 59, no. 6, pp. 2898-2905, July 2010, doi: 10.1109/TVT.2010.2047283.

[12] C. Cheng, H. Sari, S. Sezginer and Y. T. Su, "New signal design for enhanced spatial modulation with multiple constellations," 2015 IEEE 26th Annual International Symposium on Personal, Indoor, and Mobile Radio Communications (PIMRC), 2015, pp. 872-876, doi: 10.1109/PIMRC.2015.7343420.

[13] M. Carosino and J. A. Ritcey, "Performance of MIMO enhanced spatial modulation under imperfect channel information," 2015 49th Asilomar Conference on Signals, Systems and Computers, 2015, pp. 1415-1419, doi: 10.1109/ACSSC.2015.7421376.

PROJECT DETAILS

Student Details			
Student Name	Vibhuti Ravi		
Register Number	170907092	Section / Roll No	A /16
Email Address	vibhutiravi@gmail.com	Phone No (M)	7799150000
Project Details			
Project Title	Constellation Designs for improved error correction in 5G MIMO systems under Correlated Nakagami Fading		
Project Duration	4 months	Date of reporting	19.01.2021
Expected date of completion of project	2.06.2021		
Organization Details			
Organization Name	Manipal Institute of Technology, MAHE		
Full postal address with pin code	Manipal Institute of Technology, MAHE, Udupi - Karkala Rd, Eshwar Nagar, Manipal, Karnataka 576104		
Website address	https://manipal.edu/mit.html		
Supervisor Details			
Supervisor Name	Dr. Goutham Simha G D		
Designation	Assistant Professor		
Full contact address with pin code	Manipal Institute of Technology, MAHE, Udupi - Karkala Rd, Eshwar Nagar, Manipal, Karnataka 576104		
Email address	goutham.simha@manipal.edu	Phone No (M)	+91 9740773415
Internal Guide Details			
Faculty Name	Dr. Goutham Simha G D		
Full contact address with pin code	Dept. of E&C Engg., Manipal Institute of Technology, Manipal – 576 104 (Karnataka State), INDIA		
Email address	goutham.simha@manipal.edu		